Experimental Seakeeping and Uncertainty Analysis of Benchmark Ship Model in Regular Head and Beam Waves

Experimentalna analiza ispitivanja i mjerne nesigurnosti referentnog modela broda na pravilnim pramčanim i valovima u bok

Nandiko Rizal*
Institut Teknologi Sepuluh Nopember
Department of Marine Engineering
Kampus ITS - Sukolilo Indonesia
Research Center for Hydrodynamics
Technology - BRIN
E-mail: nandikorizal127@gmail.com

Dian Purnama Sari
Research Center for Hydrodynamics
Technology - BRIN
Indonesia
E-mail: dianpurnamasari173@yahoo.co.id

Beny Cahyono
Institut Teknologi Sepuluh Nopember
Department of Marine Engineering
Kampus ITS - Sukolilo, Indonesia
E-mail: Cak_beny@yahoo.com

Dedy Dwi Prastyo
Institut Teknologi Sepuluh Nopember
Departement of Statistics
Kampus ITS - Sukolilo, Indonesia
E-mail: dedy-dp@statistika.its.ac.id

Baharuddin Ali
Hydrodynamics Laboratory - BRIN
Indonesia
E-mail: baha002@brin.go.id

Erdina Arianti
Research Center for Hydrodynamics
Technology - BRIN
Indonesia
E-mail: erdina.arianti@brin.go.id

Abstract

Confidence levels of the seakeeping experiment results can be assessed through uncertainty analysis. The seakeeping experiments with a free-running model system were carried out in the manoeuvring and ocean engineering basin (MOB) at the Indonesian Hydrodynamic Laboratory (IHL) using uncertainty techniques to improve the experiment quality. The method used is the International Organization for Standardization, Guide for Uncertainty of Measurements (ISO-GUM), type A and B uncertainty, which is the foundation for the uncertainty analysis for seakeeping experiment recommendations released by the International Towing Tank Conference (ITTC). This research aims to determine the combined uncertainty value of the seakeeping experiment on a benchmark ship model with a scale of 1:62, representing the full scale of 186 meters. Seakeeping testing is carried out under head and beam waves, each with regular waves at one wave height (Hs) with three different wave periods (Tw). The experimental seakeeping result, generally, has the same tendency in each heave, pitch, and roll motion mode. The expanded uncertainty with 95% confidence level of the RAO-Heave uncertainty in all period conditions is always less than 3%, RAO-Pitch uncertainty in all period conditions is always less than 1%, and RAO-Roll uncertainty in all period conditions is always less than 1.2%. These uncertainties are quite small.

Sažetak

Razine pouzdanosti rezultata eksperimenta ispitivanja broda na valovima mogu se ustanoviti analizom mjerne nesigurnosti. Eksperimenti ispitivanja uz sustav slobodno vođenog modela provedeni su u bazenu za manevriranje i oceansko inženjerstvo (MOB) u Indonezijskom laboratoriju za hidrodinamiku (IHL) uporabom tehnika za utvrđivanje mjerne nesigurnosti za što bolju kvalitetu eksperimenta. Metoda koja se koristila u skladu je s Međunarodnom organizacijom za standardizaciju, Upute za iskazivanje mjerne nesigurnosti (ISO-GUM), tip A i B nesigurnosti, što je u skladu s preporukama za ispitivanje i analizu mjerne nesigurnosti koje su objavljene na Međunarodnoj konferenciji ITTC. Cilj je ovoga istraživanja odrediti kombiniranu mjernu nesigurnost ispitivanja na referentnom modelu broda prema ljestvici 1 : 62, gdje je zastupljena puna ljestvica od 186 m. Ispitivanje je provedeno na pramčane i valove u bok, svako s pravilnim valovima i jednake visine vala (Hs), uz tri različita perioda vala (Tw). Rezultat eksperimentalnog ispitivanja, općenito, pokazao je istu tendenciju u svakom modu podizanja, propadanja i valjanja. Proširena mjerna nesigurnost s 95% sigurnosti RAO_Heave nesigurnosti (podizanje) u svim periodima uvijek je manja od 3%, RAO-Pitch nesigurnosti (propadanje) u svim periodima uvijek je manja od 1% i RAO-Roll nesigurnosti (valjanje) u svim je periodima uvijek manja od 1.2%. Ove su mjerne nesigurnosti sasvim male.

1. INTRODUCTION / *Uvod*

It is essential to know the prediction of the seakeeping performance of a ship at the design stage, both numerical

prediction and experimental testing in wave basin. The aim is to increase navigation safety. The ship model must be tested first by some criteria, including its movement and measurements from

---

* Corresponding author

six degrees of freedom (6 DoF) in the form of heave, roll, pitch, surge, sway, and yaw. Statistical analysis of measurements is presented to determine the quality of ship movement. The measured data is also displayed in the response amplitude operator (RAO). Evaluation of the precision of any experiment or measurement, particularly seakeeping experiments, where uncertainty measurement performed/completed, is a crucial consideration. Uncertainty measurements are integral in the shipbuilding process because their analysis can identify/determine the level of certainty. Uncertainty analysis is also vital to obtain an objective indicator/benchmark for the degree of confidence that can later be used to determine the error rate in the measurement results. Confidence levels in experimental and computational research have been assessed through uncertainty analysis for years, but it has not been used for shipbuilding or offshore structures.

The recommendation from ITTC [1] is to adopt the ISO-GUM approach [2] to perform an analysis of the uncertainty of experimental results. ISO-GUM categorises uncertainty into two types: types A and B. A research study by Willink [3] summarized the principles underpinning the proposed new method of assigning uncertainties as the international standard for evaluating uncertainty in measurement and recommendation INC-1 1980. ITTC [4] compiled and recommended guidelines for representing sampling error in standardised procedures whose purpose is to benefit society itself and affiliates. Following the assessment method, ITTC published the advised steps and instructions for seakeeping testing on 7.5-02-07-02.1. by employing a technique for assessing uncertainty.

The Indonesian Hydrodynamic Laboratory (IHL) has used procedures and instructions 7.5-02-07-02.1 for the seakeeping testing uncertainty technique. IHL investigates all potential causes of uncertainty, provides realistic estimates, and prevents the reporting of erroneous test results. All elements of model geometry uncertainty, instrumentation calibration, and model testing uncertainties (free-running system and repeated measurements) are identified. Previous research on uncertainty analysis was presented at IHL as described in [5,6,7].

Previous studies have explored the measurement uncertainty of the seakeeping test, Papatzanakis et al. [8] evaluation the seakeeping performance characteristics and the circumstances impacting voyage on an onboard decision support system. Quadvlieg and Brouwer [9] explained that the presented uncertainty analysis focuses on the results of the manoeuvres, the values of overshoot angles, advance and tactical diameter, and steady turning characteristics at 35 degrees rudder angle, which are practically not influenced by any roll angles, so that it may be considered a good validation case for predictions where the roll angle is not dominant. Research by Eloot et al. [10] explained that the repetition of measurements of the seakeeping free-running was determined with several conditions to determine the distribution of measurements for all three experiments. In their recent journal, Ueno et al. [11] mentioned that the uncertainties in the hydrodynamic forces were identified, such as the surge and sway forces, yaw moment, rudder tangential and normal forces, and propeller thrust, which were relatively minimal. The reported uncertainty analysis results of the circular motion test data could be beneficial in validating data quality and reliability for modelling the ship's turning ability. Among the most reliable methods for assessing ship responsiveness is modelling vessels

turning action using a statistical equation using tank test data and hydrodynamic derivatives. ITTC [12] proposes figuring out how the experiment's uncertainty will spread. All stages use simulation to ascertain the strategy for measuring results, which will depend on the original failure being affected. Papanikolaou et al. [13] express consideration of the uncertainty associated with the vessel's seaworthiness response and wave oodles is required to assess the concept operation and to ensure safe and efficient maritime transportation. To accomplish it well, data clarification in effective bulk and stochastic load combinations using numerical models aids in the testing and evaluation of design criteria and statements in the sense of uncertainty in propulsion systems, as well as aids in the rationalisation of modelling assumptions.

The research was conducted by Remola and Rojas [14]. explained that an uncertainty analysis was carried out to determine roll attenuation parameters because roll attenuation when testing seakeeping on ships or platforms is significant. The uncertainty associated with timing measurements can be easily determined from sample rates and uncertainties associated with angle measurements, depending on the device. According to Sprenger et al. [15] tests of propulsion and rudder force in wave water conditions and evaluation of ship manoeuvrability in wave water conditions compared to calm water conditions are approaches that cause significant safety problems for some types of ships, as the ship's manoeuvrability under challenging situations may no longer be adequate. Qiu et al. [16] developed combined experimental and numerical methods for measuring uncertainties in model geometry, model mass properties, model locations, and the set-up of mooring systems. It was found that the uncertainty due to the model geometry is negligible. However, due to the mass nature of the model, it may be significant for roll decay. Gaps in uncertainty cause large uncertainties in all measurement results. Parunov et al. [17] explained that the uncertainty metric is the frequency-independent model error. The study has two aims: to acquire valuable information regarding damage modelling in the seakeeping analysis of damaged ships and to contribute to a rational approach for defining linear seakeeping tools. The analysis is performed for vertical motions, vertical and horizontal global wave load components, and torsional moments. In addition to Parunov et al. [18] a study was conducted to assess the level of doubt in linear transfer functions caused by various seakeeping codes and how that uncertainty affects extreme vertical wave bending moments over a long period. For each technique average regarding the scientific results, uncertainty estimates are computed for each seakeeping code about the average of the associated method. Continuing estimations of the upward wave deflections at midship have significant uncertainties produced using various seakeeping codes. Parunov et al. [19] presented general concepts and modelling of the uncertainty in linear and non-linear low-frequency wave-induced loads. The relevance of these uncertainties for practical applications in the shipping industry as the rule development process, ship structural reliability analysis, uncertainty-based decision support systems, structural health monitoring, and consequently ship digital twins are addressed. The study is performed within the ISSC (International Ship and Offshore Structures Congress) and ITTC Joint Committee promoting a common understanding of matters related to modelling uncertainties in the description of waves and wave-induced responses of marine structures. Oršić and Dejhalla

[20] explained that estimate of ship seakeeping characteristics is critical due to the high motion requirements in terms of all the extra demands for sailing convenience and ship equipment efficiency. High amplitudes of ship movement on waves can endanger people, equipment, and cargo, and, in extreme cases, ship construction can be cracked. Zakki et al. [21] conducted research to create a catamaran hull form for the hull of a fish processing vessel. In terms of hull resistance performance, the analysis revealed that the catamaran hull form outperformed the monohull with a service speed of more than 23 knots. The analysis results for intact stability showed that the catamaran hull form has better intact stability characteristics than the monohull. The catamarans' hull's large demi-hull spacing can be reduced. Shaw's [22] methods for evaluating uncertainties in experimental data and predictions made using these data, with implementation in R.

Previous research on type B uncertainty analysis was described in [23], while the current study aims to identify the source of type A uncertainty. Type A uncertainty represents random uncertainty evaluated by statistical methods based on repeated testing. The measurement of seakeeping performance was carried out three times with repeated measures. Any uncertainty to be determined and presented will have an error/uncertainty of results. For this reason, the probability of correctness of the conjecture for experimental error is also known as uncertainty.

2. RESEARCH METHOD / *Istraživačka metodologija*

Regular waves were used in seakeeping free-running experiments. This technology uses a driving system that can move with six levels of liberty under control. Motion tracking equipment will identify the target sensor that monitors model movement data. It is envisaged that this system will provide a more accurate description of the ship's movement during operation. Six motion detector cameras, 6 DoF, and a wave height sensor (WHS) were used to measure the altitude of the wave and motion at 6 DoF.

Figure 1 depicts the model utilised in this seakeeping test. The model's construction material was wood, coated in glass thread, and painted to create a slick area. The dimensions were verified on a 3-axis measurement table during the modelling phase. The primary sizes of the models are described in Table 1 below.

Table 1 Dimensions of the principal benchmark models
Tablica 1. Dimenzije osnovnih referentnih modela

Particulars	Symbol	Unit	Value Model
Scale			**1:62**
Length overall	*LOA*	m	3,000
Length between perpendicular	*Lpp*	m	2,930
Breadth	*B*	m	0,500
Depth	*H*	m	0,119
Draught (full load)	*T*	m	0,077

The method recommended by ISO-GUM classifies elements of uncertainty into two categories: type A and type B, based on how they are evaluated.

2.1. Uncertainty of type A / *Mjerna neizvjesnost Tipa A*

Type A uncertainty represents random uncertainty evaluated by statistical methods based on repeated measurements. The benchmark model's seakeeping performance was measured three times with repeated experiments under regular wave conditions. The test program data can be seen in Table 2 below.

Table 2 Wave conditions
Tablica 2. Stanje valova

Wave height (*Hs*) (meter)	Wave period (*Tw*) (second)	Wave type
3.50	8.30	Regular
	10.70	
	12.50	

The test was conducted in the manoeuvring and ocean engineering basin (MOB) at IHL with a free-running model at *Vs* = 12 knots. The Recommended Practices and Guidelines from the ITTC Rev. 06 of 7.5-02-07-02.1, 2017.

An optical wireless detection device records the method to gain access to motion data. Motion detection instruments will identify the spot detector mounted on the model and provide additional documentation in model motion data. IHL performs an uncertainty calculation on the ITTC-required benchmark seakeeping model to conduct the verification method.
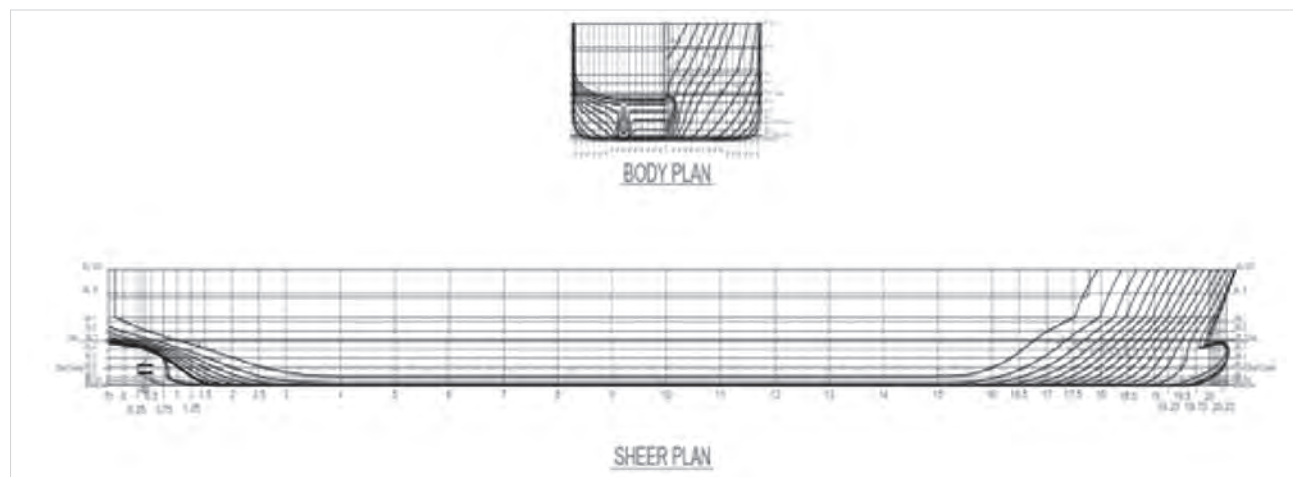

Figure 1 Lines Plan model benchmark.
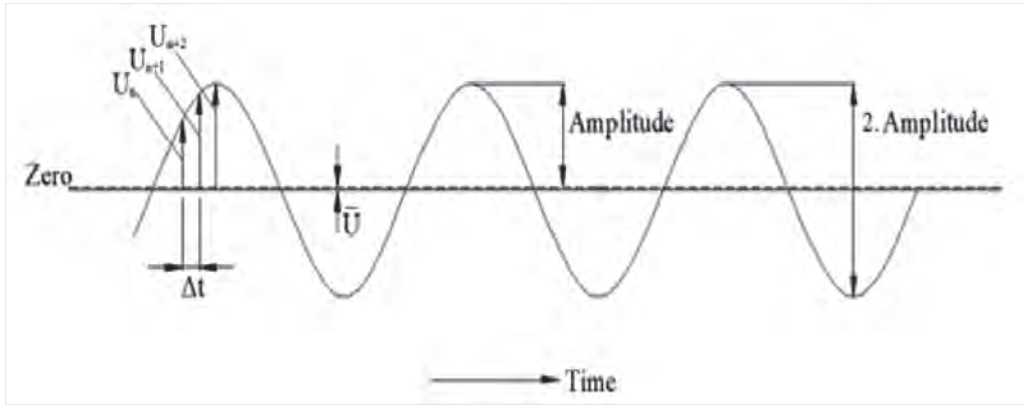*Slika 1. Plan linija referentnog modela*

Figure 2 Regular wave signal
Slika 2. Signal pravilnog vala

2.1.1. Axis systems and analysis of data / *Sustavi osi i analiza podataka*

To carry out these measurements, the right-hand axis system is used to define them. The model is moving in a positive direction, as shown in the following:

X denotes an upward surge.

Y is swaying to the harbour sides.

Z is a heave or upward motion.

For rotary motion, a positive clockwise direction is specified for each rotary axis.

φ is rolling about the x-axis.

θ is pitch concerning the y-axis.

ψ is yaw about the z-axis.

Before testing, a zero reading was carried out for all channels. Then the wave generation starts, and after a while, until the transient effect disappears, the measurement begins. The signal description is shown in Figure 2 below in regular signal processing for the statistical analysis.

Measurement of fast signal oscillations with a sampling frequency of 50 Hz data. Regular wave test results are tabulated in statistical analysis using various signal parameters that have been measured, where the amplitude is generated from the amplitude spectrum via Fast Fourier Transform (FFT).

In the axis, the RAO displays the measurement outcomes, giving the ratio value between the input wave amplitude and the output signal amplitude for each mode of motion. The formula is defined as follows:

$$\text{RAO Heave} = \frac{\zeta_z}{\zeta_a} \tag{1}$$

ζ_z is amplitude heave (m), ζ_a is amplitude wave (m)

$$\text{RAO Pitch} = \frac{\zeta_\theta \lambda}{360 \zeta_a} \tag{2}$$

ζ_θ is amplitude pitch (deg), λ is the wavelength (m), ζ_a is amplitude wave (m)

$$\text{RAO Roll} = \frac{\zeta_\phi \lambda}{360 \zeta_a} \tag{3}$$

ζ_ϕ is amplitude roll (deg), λ is the wavelength (m), ζ_a is amplitude wave (m)

As for the abscissa in the non-dimensional λ/Lpp, as depicted in Equation 4.

$$\lambda = \frac{g}{(2\pi) Tw^2} \tag{4}$$

λ is the wavelength (m), g is 9.81 (m/sec²), *Tw* is wave period (sec), and *Lpp* is the *Lpp* ship (m).

2.1.2. Type A uncertainty evaluation / *Evaluacija mjerne nesigurnosti Tipa A*

Type A uncertainty is evaluated by using free-running seakeeping tests and repeated measurements. Prepare data on seakeeping free-running test results for benchmark ship models and repeated tests in the form of:

- Model speed (*V* (m/s)).
- Wave elevation (amplitude ζ_a (m), period *Tw* (s)).
- Wavelength λ/Lpp.
- Model heading direction (yaw motion (deg)).
- The Heave and Pitch values are displayed as a non-dimensional response amplitude operator (RAO) of the Heave and Pitch motions (for heading 180⁰).
- The Roll value is displayed as a non-dimensional response amplitude operator (RAO) of the Roll motion (for 90⁰ headings).

From each component, the uncertainty calculation is carried out

u_v is uncertainty regarding model velocity *V*

u_{ζ_a} is uncertainty regarding the wave amplitude ζ_a.

$u_{\lambda/Lpp}$ is uncertainty regarding wavelength λ/L_{pp}.

u_ψ is uncertainty regarding yaw.

u_z is uncertainty regarding non-dimensional RAO-Heave.

u_θ is uncertainty regarding non-dimensional RAO-Pitch.

u_ϕ is uncertainty regarding non-dimensional RAO-Roll.

The uncertainty calculation is influenced by two factors, namely statistical analysis uncertainty (u_A) and equipment (wave probe) uncertainty (u_B). The two uncertainty values are added together to become the standard uncertainty (*u*) using equation (5).

$$u = \sqrt{u_A^2 + u_B^2} \tag{5}$$

In general, the uncertainty measurement formulation of the wave amplitude (u_{ζ_a}), model velocity (u_v) and non-dimensional yaw (u_ψ) can be written as in Eq (6).

$$u_x = \frac{\sqrt{\frac{1}{N-1} \sum_{i=1}^{N}(x_i - \bar{x})^2}}{\bar{x}} \tag{6}$$

The period of the T_W wave correlates with the wavelength λ which can be formulated $\lambda = \frac{g}{(2\pi)Tw^2}$ while in non-dimensional form it is written as λ/Lpp with the uncertainty calculation ($u_{\lambda/Lpp}$) which can be seen in the equation 7.

$$u_{\lambda/Lpp} = \sqrt{(\frac{1}{Lpp})^2 u^2(\lambda) + (\frac{\lambda}{Lpp^2})^2 u^2(Lpp)} \tag{7}$$

The uncertainty calculation for RAO-Heave motion (u_z) is influenced by two factors, namely statistical analysis uncertainty (u_A) and equipment uncertainty (qualisys surface motion camera) (u_B). The two uncertainty values are added together to form u standard uncertainty using equation (5). Uncertainty statistical analysis of heave motion in non-dimensional form is obtained by the equation 8.

$$u_z = \sqrt{\left(\frac{1}{\zeta_a}\right)^2 u^2(z_a) + \left(\frac{z_a}{\zeta_a^2}\right)^2 u^2(\zeta_a)} \tag{8}$$

Calculating uncertainty for RAO-Pitch motion (u_θ) in non-dimensional form is obtained by equation (9).

$$u_\theta = \sqrt{\left(\frac{\overline{\lambda}}{360\zeta_a}\right)^2 u^2(\theta_a) + \left(\frac{\theta_a\lambda}{360\zeta_a^2}\right)^2 u^2(\zeta_a) + \left(\frac{\overline{\theta_a}}{360\zeta_a^2}\right)^2 u^2(\lambda)} \tag{9}$$

Calculation of uncertainty for RAO-Roll motion ($u_\emptyset$) in non-dimensional form is obtained by equation (10).

$$u_\phi = \sqrt{\left(\frac{\overline{\lambda}}{360\zeta_a}\right)^2 u^2(\emptyset_a) + \left(\frac{\overline{\emptyset_a}\lambda}{360\zeta_a}\right)^2 u^2(\zeta_a) + \left(\frac{\overline{\phi_a}}{360\zeta_a}\right)^2 u^2(\lambda)} \tag{10}$$

2.1.3. Combined uncertainty evaluation (u_c) / Kombinirana evaluacija mjerne nesigurnosti

The combined uncertainty of the result of one measurement is derived from the uncertainty of a number of other quantities. The combined uncertainty as calculated through the law of the uncertainty propagation.

Calculating the combined uncertainty value (u_c) of all causes of uncertainty using equation (11).

$$u_c = \sqrt{\sum_{i=1}^{n} u_i^2} \tag{11}$$

2.1.4. Expanded uncertainty evaluation (U) / Proširena evaluacija mjerne nesigurnosti

The expanded uncertainty calculated as the combined uncertainty must be multiplied by the coverage factor to get the overall uncertainty value. The total uncertainty is called extended uncertainty. In hydrodynamic testing, k with a 95% confidence level. All ITTC results will be reported with expanded uncertainty at the 95% confidence level.

Carrying out uncertainty calculations is expanded using equation (12).

$$U = k\,u_c \tag{12}$$

Table 3 Aspect for every degree of trust
Tablica 3. Aspekt za svaki stupanj sigurnosti

Degree of trust (%)	Aspect
50.00	0.676
68.27	1.000
90.00	1.645
95.00	1.960
99.00	2.576
99.73	3.000

Source: ITTC., (2017), Recommended Procedures and Guidelines 7.5-02-07-02.1, Rev. 06, Seakeeping Experiments, p. 13

2.2. Uncertainty of type B / Mjerna nesigurnost Tipa B

The degree of uncertainty derived using methodologies other than facts and figures and the information currently available is known as the standard type B uncertainty. Type B uncertainty standard consists of calibration certificates, specifications of measurement tools, handbooks, and data records. As mentioned above, uncertainty in the geometry and calibration of the instrumentation is the root of type B uncertainty in seakeeping test results in IHL. Table 4 displays the categories B of uncertainty.

Table 4 Categories B of uncertainty
Tablica 4. Kategorije B mjerne nesigurnosti

Items	Categories B of uncertainty
Geometry	Specifications of the marking table
Mass distribution model	Specifications of The stopwatch and Hanging electric scale.
Calibration instrumentation	Specifications of detectors and equipment: WHS, Six DoF motion camera, and The wand
Seakeeping free running test	-
Repeated measurement	-

3. RESULT AND DISCUSSION / Rezultat i rasprava

The range of uncertainty (u) in the numbers acquired from each test also impacted the relevance of the evaluation results. The test's relevant factors could be broken down into several other categories, as demonstrated in Figure 3, specifically, the geometry uncertainty, calibration uncertainty, free-running method, and repeated measurement. Additionally, the combination uncertainty can be determined after acquiring this uncertainty.
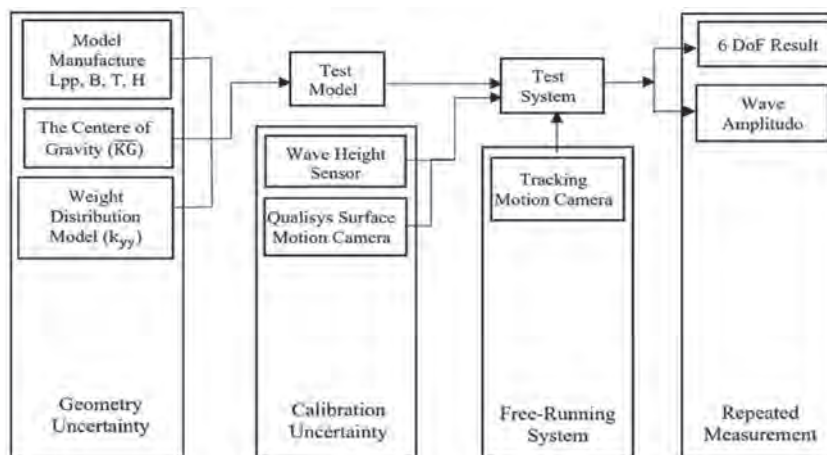

Figure 3 Factors that influence seakeeping testing uncertainty [23].
Slika 3. Čimbenici koji utječu na mjernu nesigurnost ispitivanja broda [23]

3.1. Geometry uncertainty / *Mjerna nesigurnost geometrije modela*

The uncertainty estimates for model geometry was: model geometry *Lpp* is length, *B* is the breadth, *T* is draft, and *H* is depth were checked in the marking table as shown in Figures 4a and 4b, Weight distribution model (k_{yy}) was reviewed in the oscillation table, as shown in Figures. 5a and 5b. At the same time *KG* positions were essential for the seakeeping experiment, as a product of the inclining test.

3.2. Calibration uncertainty / *Mjerna nesigurnost kalibracije*

The calibration's level of uncertainty, specifically of the wave height sensor's (WHS) U_{whs}, regular wave calibration with WHS as shown in Figure 6, and calibration result chart for WHS as shown in Figure 7, while motion cameras' 6 DoF (Qt) calibration results were collected from reports on the equipment's calibration results. For each experiment, motion cameras with 6 DoF were calibrated at the headings of 180⁰ and 90⁰. As shown in Figure 8, the calibration position for four motion cameras is 6 DoF for heading 90⁰, and the calibration position for six motion cameras is 6 DoF for heading 180⁰, as shown in Figure 9.

The wand, electric hanging, stopwatch, and marking table were gained from each calibration's outcomes for each piece of equipment performed by external parties, namely Qualisys, Caltesys, and MIDC, Ministry of Industry, as shown in Table 5.

| (a) | (b) |

Figures 4a and 4b The main dimensions of the benchmark ship model were checked on a 3-axis measurement table
Slike 4a i 4b. Osnovne dimenzije referentnog modela broda provjerene su na mjernom stolu s 3 osi

Source: [23]

| (a) | (b) |

Figures 5a and 5b Measurement of mass distribution model (k_{yy}) in the oscillation table
Slike 5a i 5b. Mjerenje modela distribucije mase (k_{yy}) na oscilacijskom stolu

Source: [23]

Table 5 Equipment used before the seakeeping experiment
Tablica 5. Oprema korištena prije eksperimentalnog ispitivanja

Items	Capacity	Measurement Uncertainty	Traceability
The wand	Length 1000 mm	± 0,1 mm (2σ)	factory calibration (Qualisys-certificate calibration)
Electric hanging	600kg	± 0,13 Kg	Via LK-032-IDN, calibration results can be detected by the International System of Units (SI)
Stopwatch	10 minutes	± 0,65 seconds	Via LK-032-IDN, calibration results can be detected by the International System of Units (SI)
3-axis measurement table		$U_{95\%}$ = 15 m (k = 2)	This instrument is calibrated with Laser Interferometer XL-10 No. Series: H43156 traceable to International System (SI) via Renishaw

The results of the calculation of the uncertainty of geometry, mass distribution, and uncertainty of the calibration of the instrument from previous work were published in [23, pages 12, 13], in Appendix A.

Figure 6 Regular wave calibration with WHS
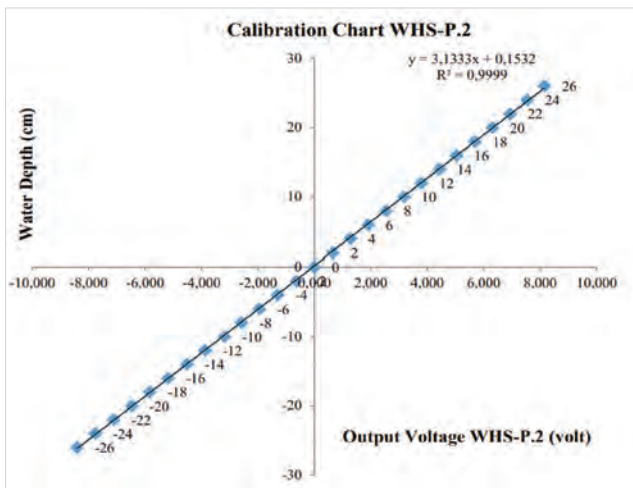*Slika 6. Kalibracija pravilnog vala s WHS-om*

Figure 7 The calibration chart results for the WHS [23]
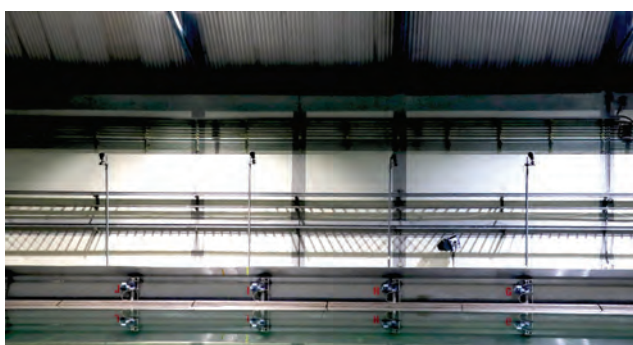*Slika 7. Rezultati kalibracijske karte za WHS [23]*

Figure 8 Four motion detector cameras with six degrees of freedom at a heading of 90^0
Slika 8. Četiri kamere detektora pokreta sa šest stupnjeva za smjer od 90⁰

Figure 9 Six motion detector cameras with six degrees of freedom at a heading of 180^0
Slika 9. Šest kamera detektora pokreta sa šest stupnjeva za smjer od 180⁰

3.3. Seakeeping free-running system testing and repeated measurements / *Testiranje sustava slobodne vožnje i ponovljena mjerenja*
3.3.1. Seakeeping test results / *Rezultati testa ispitivanja*

The outcomes of the free-running seakeeping tests (Running-1, 2, and 3) for pitching and heaving at a heading of 180° on the benchmark ship model are shown in Tables 6 and 7, the units in Table 6 and 7 refer to equations 1, 2, and 4. The graphics of RAO-Heave and RAO-Pitch are shown in Figures 10 and 12. The abscissa and ordinate units refer to equations 1, 2, and 4. A photograph of test conditions is shown in Figures 11 and 13.

Table 6 RAO-Heave benchmark ship model seakeeping test results, heading 180⁰
Tablica 6. Rezultati testa ispitivanja referentnog modela broda RAO-Heave, smjer 180⁰

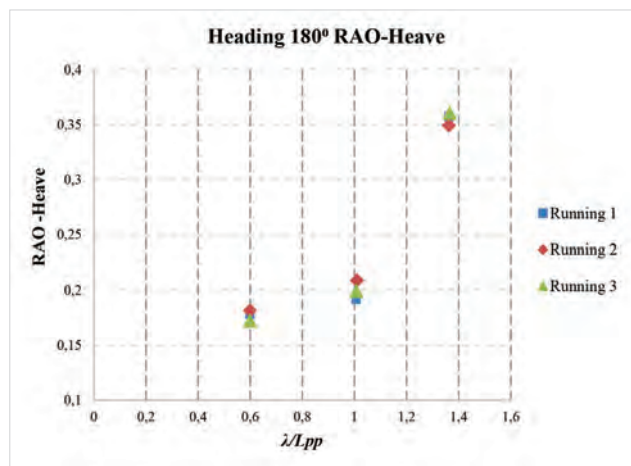| Running -1		Running - 2		Running - 3	
λ/Lpp	RAO-Heave	λ/Lpp	RAO-Heave	λ/Lpp	RAO-Heave
0.599	0.178	0.599	0.182	0.598	0.172
1.007	0.192	1.010	0.209	1.008	0.199
1.363	0.357	1.363	0.350	1.366	0.361

Figure 10 Results of running 1, 2, and 3 RAO-Heave measurements
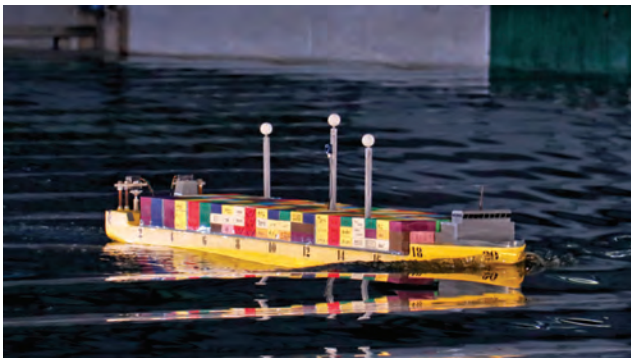*Slika 10. Rezultati vožnje 1, 2 i 3 RAO-Heave mjerenja*

Figure 11 Seakeeping experiment at heading 180⁰
Slika 11. Ispitivanje uz smjer 180⁰

The outcomes of the free-running seakeeping tests (Running-1, 2, and 3) for the roll at heading 90⁰ on the benchmark ship model are shown in Table 8, the units in Table 8 refer to equations 3 and 4. The graphic RAO-Roll is shown in Figure 14, The abscissa and ordinate units refer to equations 3 and 4. Photographs of test conditions are shown in Figure 15.

Table 8 RAO-Roll benchmark ship mode seakeeping trial results, heading 90⁰
Tablica 8. Rezultati probnog ispitivanja referentnog modela broda RAO-Roll, smjer 90⁰

Running -1		Running - 2		Running - 3	
λ/Lpp	RAO-Roll	λ/Lpp	RAO-Roll	λ/Lpp	RAO-Roll
0.598	5.577	0.598	5.338	0.599	5.444
1.007	2.049	1.007	1.972	1.007	2.031
1.364	1.221	1.363	1.249	1.364	1.259

Table 7 RAO-Pitch benchmark ship model seakeeping trial results, heading 180⁰
Tablica 7. Rezultati probnog ispitivanja referentnog modela broda RAO-Pitch, smjer 180⁰

Running -1		Running - 2		Running - 3	
λ/Lpp	RAO-Pitch	λ/Lpp	RAO-Pitch	λ/Lpp	RAO-Pitch
0.599	0.207	0.599	0.213	0.599	0.199
1.007	0.611	1.010	0.615	1.007	0.606
1.363	0.910	1.363	0.883	1.366	0.911

Figure 14 Results of running 1, 2, and 3 RAO-Roll measurements.
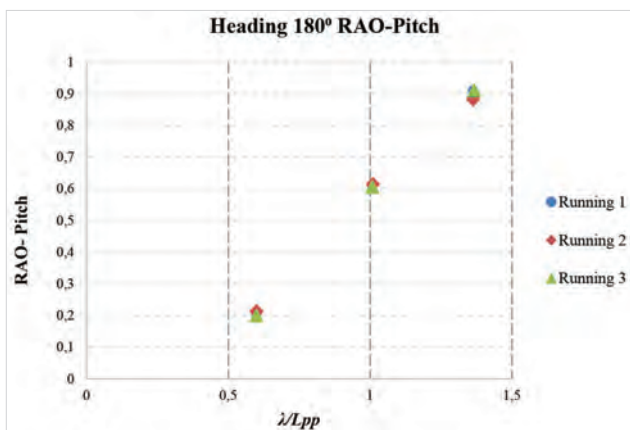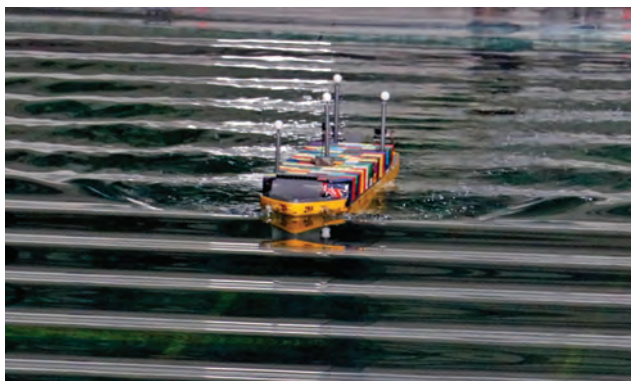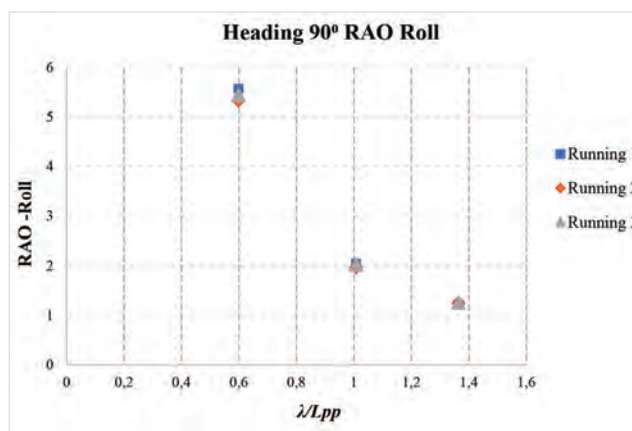*Slika 14. Rezultati vožnje 1, 2 i 3 RAO-Roll mjerenja*

Figure 12 Results of running 1, 2, and 3 RAO-Pitch measurements
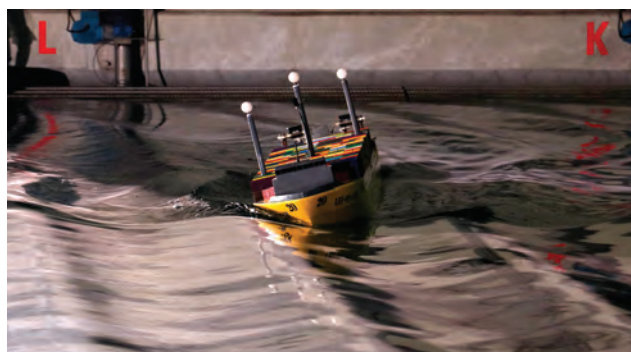*Slika 12. Rezultati vožnje 1, 2 i 3 RAO-Pitch mjerenja*

Figure 15 Seakeeping experiment at heading 90⁰.
Slika 15. Ispitivanje uz smjer 90⁰

3.3.2. Calculation of seakeeping free-running system uncertainties and repeated measurements / *Izračun mjernih nesigurnosti sustava slobodne vožnje i ponovljena mjerenja*

The uncertainty of testing the seakeeping free-running and repeated measurement three times for pitching and heaving movements at a heading of 180⁰ is shown in Table 9. The uncertainty of rolling movements at 90⁰ is shown in Table 10. The calculation refers to equations 5, 6, 7, 8, 9, and 10.

Figure 13 Seakeeping experiment at heading 180⁰
Slika 13. Ispitivanje uz smjer 180⁰

Table 9 The uncertainty for RAO-Heave and RAO-Pitch motion at heading 180⁰

Tablica 9. Mjerna nesigurnost za RAO-Heave i RAO-Pitch uz smjer 180⁰

Wave period (Tw)	Uncertainty of the Wave Amplitude [%] (u_{ζ_a})	Uncertainty of Model Speed [%] (u_v)	Uncertainty Wavelength λ/Lpp [%] ($u_{\lambda/Lpp}$)	Uncertainty Yaw [%] (u_ψ)	Uncertainty non-dimensional RAO-Heave [%] (u_z)	Uncertainty non-dimensional RAO-Pitch [%] (u_θ)
8.3 sec	0.058	0.336	0.017	0.001	1.343	0.001
10.7 sec	0.047	0.139	0.091	0.005	1.354	0.002
12.5 sec	0.045	0.078	0.117	0.002	1.343	0.003

Table 10 The uncertainty for RAO-Roll motion at a beam sea (90⁰ wave heading).

Tablica 10. Mjerna nesigurnost za RAO-Roll kretanje uz bočne valove (smjer valova 90⁰)

Wave period (Tw)	Uncertainty of the Wave Amplitude [%] (u_{ζ_a})	Uncertainty of Model Speed [%] (u_v)	Uncertainty Wavelength λ/Lpp [%] ($u_{\lambda/Lpp}$)	Uncertainty Yaw [%] (u_ψ)	Uncertainty non-dimensional RAO-Roll [%] ($u_\emptyset$)
8.3 sec	0.045	0.154	0.007	0.001	0.007
10.7 sec	0.044	0.460	0.013	0.002	0.005
12.5 sec	0.044	0.199	0.026	0.006	0.004

The uncertainty calculation for the combination of RAO-Heave, RAO-Pitch and RAO-Roll refers to equation 11.

Table 11 The combined uncertainty of RAO-Heave and RAO-Pith motion at a heading of 180⁰.

Tablica 11. Kombinirana mjerna nesigurnost RAO-Heave i RAO-Pitch kretanja uz smjer 180⁰

Wave period (Tw)	Combination uncertainty For RAO-Heave [%] (u_{cz})	Combination uncertainty for RAO-Pitch [%] ($u_{c\theta}$)
8.3 sec	1.435	0.505
10.7 sec	1.416	0.415
12.5 sec	1.403	0.406

Table 12 The combined uncertainty for RAO-Roll motion at a heading of 90⁰

Tablica 12. Kombinirana mjerna nesigurnost RAO-Roll kretanja uz smjer 90⁰

Wave period (Tw)	Combination uncertainty for RAO-Roll [%] ($u_\emptyset$)
8.3 sec	0.405
10.7 sec	0.594
12.5 sec	0.425

Calculation of the expanded uncertainty of RAO-Heave, RAO-Pitch and RAO-Roll refers to equation 12.

The uncertainty calculation as reported in Table 13 shows that with 95% confidence level (expanded uncertainty) the RAO-Heave uncertainty in all period condition always less than 3%, RAO-Pitch uncertainty in all period condition is always less than 1%, and RAO-Roll uncertainty in all period condition always less than 1.2%. These uncertainties are quite small.

4. CONCLUSION / *Zaključak*

The benchmark ship model, with a 1:62 scale ratio, was subjected to seakeeping experiments under free-running conditions at a regular wave height of Hs = 3.5 meters at headings of 180⁰ and 90⁰. The periods of the waves (Tw) vary from 8.3, 10.7, and 12.5 seconds. The research aims to determine the combined and expanded uncertainty value of the seakeeping experiment on a benchmark ship model at three seakeeping free-running tests.

The seakeeping tests show that heave and pitch movements have dominant motions at head seas. In contrast, roll motion is dominant at beam seas. In seakeeping testing on the benchmark ship model, it was found that running-1 to running-2 and running-3 generally have the same tendency in each heave, pitch and roll motion at three different wave periods. Moreover, the result of RAO heave, pitch, and roll values has small discrepancies along three free-running tests. So, it can be concluded that the test results are promising and feasible. In addition, the results of the uncertainty calculation of the combination of RAO heave, pitch, and roll values show that the combined uncertainty is in the range of 0.4-0.6%. The expanded uncertainty with 95% confidence level of the RAO-

Table 13 The extended uncertainty for RAO-Heave, RAO-Pitch and RAO-Roll movements

Tablica 13. Proširena mjerna nesigurnost za RAO-Heave, RAO-Pitch i RAO-Roll kretanje

Wave period (Tw)	Combination Uncertainty [%] (u_c)			Confidence Level Factor (k)	Expanded Uncertainty [%] (U)		
	RAO Heave (u_{cz})	RAO Pitch ($u_{c\theta}$)	RAO Roll ($u_\emptyset$)		RAO Heave (u_z)	RAO Pitch (u_θ)	RAO Roll ($u_\emptyset$)
8.3 sec	1.435	0.505	0.405	1.96	2.813	0.989	0.794
10.7 sec	1.416	0.415	0.594	1.96	2.776	0.812	1.164
12.5 sec	1.403	0.406	0.425	1.96	2.749	0.796	0.833

Heave uncertainty in all period conditions is always less than 3%, RAO-Pitch uncertainty in all period conditions is always less than 1%, and RAO-Roll uncertainty in all period conditions is always less than 1.2%. These uncertainties are quite small.

Conflict of interest: None.
Author contributions: All authors have accepted responsibility for the entire content of this manuscript and approved its submission.

Acknowledgement / *Zahvala*

REFERENCES / *Literatura*

[1] ITTC. (2008). ITTC-Recommended Procedures and Guidelines: Guide in the Expression of Uncertainty in Experimental Hydrodynamic, 7.5-02-01-01, Revision 01, 1-17. https://ittc.info/media/1569/75-02-01-01.pdf

[2] JCGM. (2008). JCGM 100:2008, Evaluation of Measurement Data-Guide to the Expression of Uncertainty in Measuremen. 1st ed., 1-134. https://www.bipm.org/en/committees/jc/jcgm/publications

[3] Willink, R. (2016). What Can We Learn from the GUM of 1995?. *Journal of Measurement*, 91, 692-698. https://doi.org/10.1016/j.measurement.2016.02.020

[4] ITTC. (2017). ITTC-Recommended Procedures and Guidelines: Seakeeping Experiments, 7.5-02-07-02.1, Rev. 06, pp. 1-28. https://www.ittc.info/media/8101/75-02-07-021.pdf

[5] Purnamasari, D., Utama, I. K. A. P., Suastika, I. K. & Thomas, G. A. (2020). Application of Kalman Filter to the Uncertainty of Model Resistance Data Obtained from Experiment. *Journal of Engineering Science and Technology*, 15(2), 1455-1465. https://discovery.ucl.ac.uk/id/eprint/10088338/

[6] Purnamasari, D., Utama, I. K. A. P., Suastika & I. K. (2020). Verification and Validation of a Resistance Model for Tanker 17.500 DWT. *Journal of Marine Science and Technology*, 28(1), 18-24. https://doi.org/DOI: 10.6119/JMST.202002_28(1).0003

[7] Utama, I. K. A. P., Purnamasari, D., Suastika, I. K., Nurhadi & Thomas, G. A. (2021). Toward Improvement of Resistance Testing Reliability. *Journal of Engineering and Technological Sciences*, 53(2), 197-212. https://doi.org/10.5614/j.eng.technol.sci.2021.53.2.1

[8] Papatzanakis, G. I., Papanikolaou, A. D. & Liu, S. (2012). Optimization of Routing Considering Uncertainties. *Journal of Marine Science and Application*, 11, 10-17. https://doi.org/10.1007/s11804-012-1100-y

[9] Quadvlieg, F. H. H. A. & Brouwer, J. (2011). KVLCC2 benchmark data including uncertainty analysis to support manoeuvring predictions. Proceeding of the IV International Conference on Computational Methods in Marine Engineering, Lisbon, Portugal. 325-338. https://hdl.handle.net/2117/333239

[10] Eloot, K., Delefortrie, G., Vantorre, M. & Quadvlieg, F. (2015). Validation of ship manoeuvring in shallow water through free-running tests. Proceeding of the ASME 34th International Conference on Ocean, Offshore and Arctic Engineering, 7(11), 1-11. St. John's, Newfoundland, Canada. https://doi.org/10.1115/OMAE2015-41912

[11] Ueno, M., Yoshimura, Y., Tsukada, Y. & Miyazaki, H. (2009). Circular Motion Tests and Uncertainty Analysis for Ship Maneuverability. *Journal of Marine Science and Technology*, 14, 469-484. https://doi.org/10.1007/s00773-009-0065-2

[12] ITTC. (2014). ITTC - Recommended Procedures and Guidelines: Uncertainty Analysis for Free Running Model Tests, 7.5-02-06-05, Revision 0, 1-15. https://ittc.info/media/4142/75-02-06-05.pdf

[13] Papanikolaou, A., Mohammed, E. A. & Hirdaris, S. E. (2014). Stochastic Uncertainty Modelling for Ship Design Loads and Operational Guidance. Journal of Ocean Engineering, 86, 47-57. https://doi.org/10.1016/j.oceaneng.2014.01.014

[14] Oliva Remola, A. & Perez Rojas, L. (2019). A Step forward towards developing an uncertainty analysis procedure for roll decay tests. Proceeding of the 17th International Ship Stability Workshop (ISSW 2019), Helsinki, Finland, 1-8. https://oa.upm.es/64913/1/INVE_MEM_2019_322382.pdf

[15] Sprenger, F., Maron, A., Delefortrie, G., Zwijnsvoorde, T. V., Hochbaum, A. C., Lengwinat, A. & Papanikolaou, A. (2017). Experimental Studies on Seakeeping and Maneuverability of Ships in Adverse Weather Conditions. *Journal of Ship Research,* 61(3), 131-152. https://doi.org/10.5957/JOSR.170002

[16] Qiu, W., Meng, W., Peng, H., Li, J., Roussetb, J. M. & Rodríguez, C. A. (2019). Benchmark Data and Comprehensive Uncertainty Analysis of Two-Body Interaction Model Tests in a Towing Tank. *Journal of Ocean Engineering*, 171, 663-676. https://doi.org/10.1016/j.oceaneng.2018.11.057

[17] Parunov, J., Ćorakh, M., Soares, C. G., Jafaryeganeh, H., Kalske, S., Lee, Y., Liu, S., Papanikolaou, A., Prentice, D., Prpić, J., Oršić, O., Ruponen & P., Vitali, N. (2020). Benchmark Study and Uncertainty Assessment of Numerical Predictions of Global Wave Loads on Damaged Ships. *Journal of Ocean Engineering*, 197, 1-24. https://doi.org/10.1016/j.oceaneng.2019.106876

[18] Parunov, J., Soares, C. G., Hirdaris, S., Iijima, K., Wang, X., Brizzolara, S., Qiu, W., Mikulić, A., Wang, S. & Abdelwahab, H. S. (2022). Benchmark Study of Global Linear Wave Loads on a Container Ship with Forward Speed. *Journal of Marine Structures*, 84, 1-20. https://doi.org/10.1016/j.marstruc.2022.103162

[19] Parunov, J., Soares, C. G., Hirdaris, S. & Wang, X. (2022). Uncertainties in Modelling the Low-Frequency Wave-Induced Global Loads in Ships. *Journal of Marine Structures*, 86, 1-21. https://doi.org/10.1016/j.marstruc.2022.103307

[20] Oršić, J. P. & Dejhalla, R. (1999). Auxiliary Seakeeping Characteristics Diagram Adapted to Ship Crew. *Naše more*, 46(1-2), 1-10.

[21] Zakki, A. F., Chrismianto, D., Windyandari, A. & Ilham, R. (2021). On the Development of Catamaran Hull Form for Fish Processing Vessel to Support Domestic Fishing Activities in Indonesia. Naše more, 68(3), 175-188. https://doi.org/10.17818/NM/2021/3.5

[22] Shaw, B. D. (2016). Uncertainty Analysis of Experimental Data with R. 1st ed. New York. https://doi.org/10.1201/9781315366715

[23] Rizal, N., Purnamasari, D., Cahyono, B., Prastyo, D. D., Ali, B. & Arianti, E. (2022). Uncertainty analysis study on seakeeping tests of benchmark model. Proceeding of The 3rd Maritime Safety International Conference (MASTIC 2022), IOP Conference Series: Earth and Environmental Science, 1081, 1-14. https://doi.org/10.1088/1755-1315/1081/1/012021

Appendix A / *Dodatak A*

Table 1 The outcome of the uncertainty type B computation
Tablica 1. Rezultat izračuna mjerne nesigurnosti tipa B

Cause of Uncertainty	Model Value	Units	Characterization of precision	Uncertainty of type A (%)	Uncertainty of type B (%)
Model *Lpp*	2,891	m	95% certainty	-	0.012
Model *B*	0,500	m	95% certainty	-	0.042
Model *T*	0,077	m	95% certainty	-	0.013
Model *H*	0,119	m	95% certainty	-	0.109
$\overline{KG}$	0,102	m	Inclining experiment	-	0.080
k_{yy}	0,693	m	Oscillation table	-	0.511
Motion cameras 6 DoF at 180 deg	-	m	Camera calibration	-	0.0003
Motion cameras 6 DoF at 90 deg	-	m	Camera calibration	-	0.009
WHS	-	m	WHS calibration	-	0.003